Stem Cell Reports, Volume *2*

Supplemental Information

Huntingtin Regulates Mammary Stem Cell Division and Differentiation

Salah Elias, Morgane S. Thion, Hua Yu, Cristovao Marques Sousa, Charlène Lasgi, Xavier Morin, and Sandrine Humbert

Supplemental Inventory

Figures S1 to S6

Figure S1. Related to Figure 1.
Shows the full-gating cascade strategy for isolation of mammary epithelial cell subpopulations and the characterization of *Cre* expression in E18.5 mammary rudiment of K5*Cre*;*Htt*$^{flox/flox}$;*R26* embryo.

Figure S2. Related to Figure 3.
Shows that HTT is expressed during pregnancy and lactation and influences apoptosis and proliferation.

Figure S3. Related to Figure 4.
Shows that HTT modulates mitotic spindle orientation in a dynein-dependent manner and regulates the dynamics of the mitotic spindle.

Figure S4. Related to Figure 5.
Shows HTT distribution during mitosis using different huntingtin antibodies targeted against distinct regions, and HTT immunoprecipitation using HTT (4C8) antibody.

Figure S5. Related to Figure 6.
Shows that HTT-Dynein interaction mediates the cortical localization of Dynein/Dynactin/NUMA/LGN complex during mitosis.

Figure S6. Related to Figure 7.
Shows that astral microtubules mediate the localization of Dynein/Dynactin/NUMA/LGN complex during mitosis.

Table S1. Related to Figure S1 and S2.
Shows the epithelial markers used in the study.

Supplemental Movie Legends

Movies S1 and S2. Related to Figure S3.
Show mitotic spindle positioning in Control and si-HTT1-transfected cells.

Movies S3 and S4. Related to Figure 6.
Show Dynein spatial distribution in Control and si-HTT1-transfected cells.

Movies S5 and S6. Related to Figure 6.
Show LGN spatial distribution in Control and si-HTT1-transfected cells.

Extended Experimental Procedures

Statistical Analyses

Supplemental References

Supplemental Figures

Figure S1

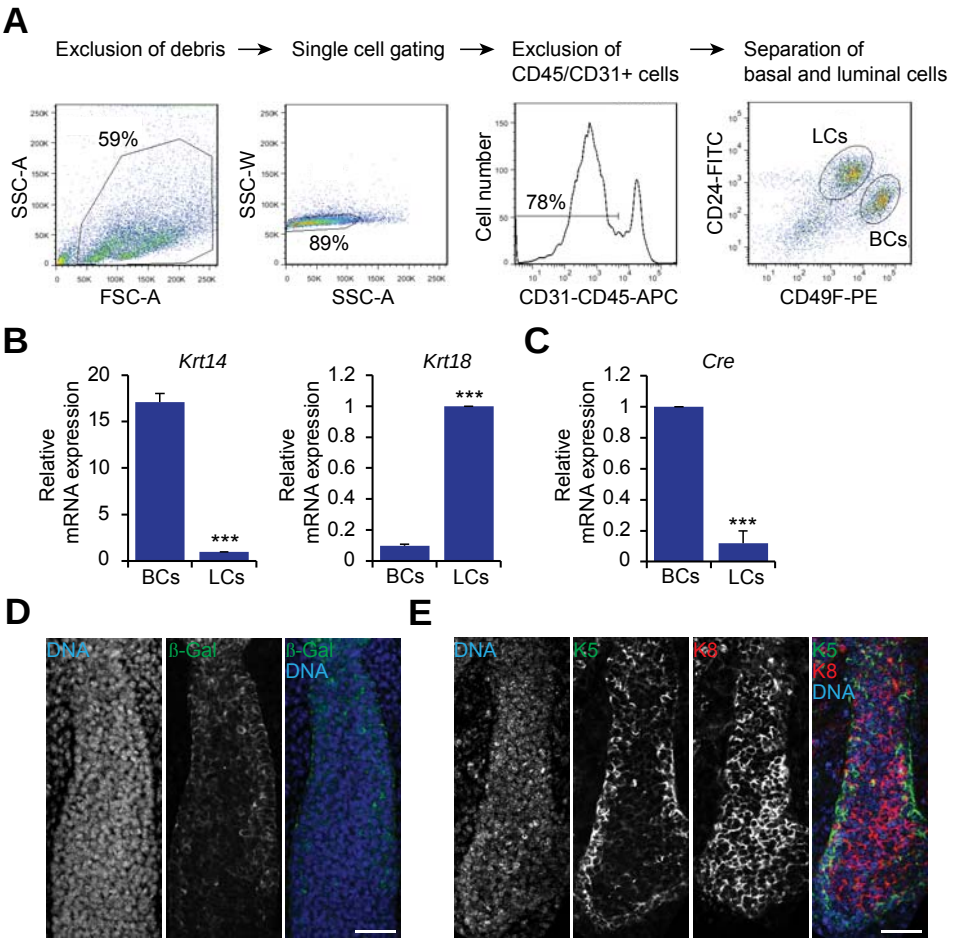

Figure S1. Related to Figure 1

(A) Gating cascade. Samples were gated on forward and side scatter (FSC/SSC) to exclude debris and single cells were isolated using time-of-flight analysis on both FSC and SSC. $CD45^+$ leukocytes and $CD31^+$ endothelial cells were removed and the total epithelial cells were gated on a CD24/CD49F plot. Epithelial subpopulations were isolated from the total epithelial cells.

(B) Quantitative real-time reverse-transcription PCR (RT-qPCR) analysis of *Krt14* and *Krt18* in basal and luminal cell populations isolated from 12-week-old virgin control mouse mammary gland. The values were normalized to *hprt* and *β-actin*.

(C) RT-qPCR analysis of *Cre* in basal and luminal cell populations isolated from 12-week-old virgin mutant mouse mammary gland. The values were normalized to *hprt* and *β-actin*.

(D) Mammary rudiment from an E18.5 female K5*Cre*;*Htt*$^{flox/flox}$;*R26* embryo stained for β-galactosidase (green) and counterstained with DAPI (DNA).

(E) Mammary rudiment from an E18.5 female K5*Cre*;*Htt*$^{flox/flox}$;*R26* embryo stained for keratin 5 (K5, green) and keratin 8 (K8, red) and counterstained with DAPI (DNA).

All scale bars, 50 μm. Error bars, SEM. *** $p<0.001$.

Figure S2

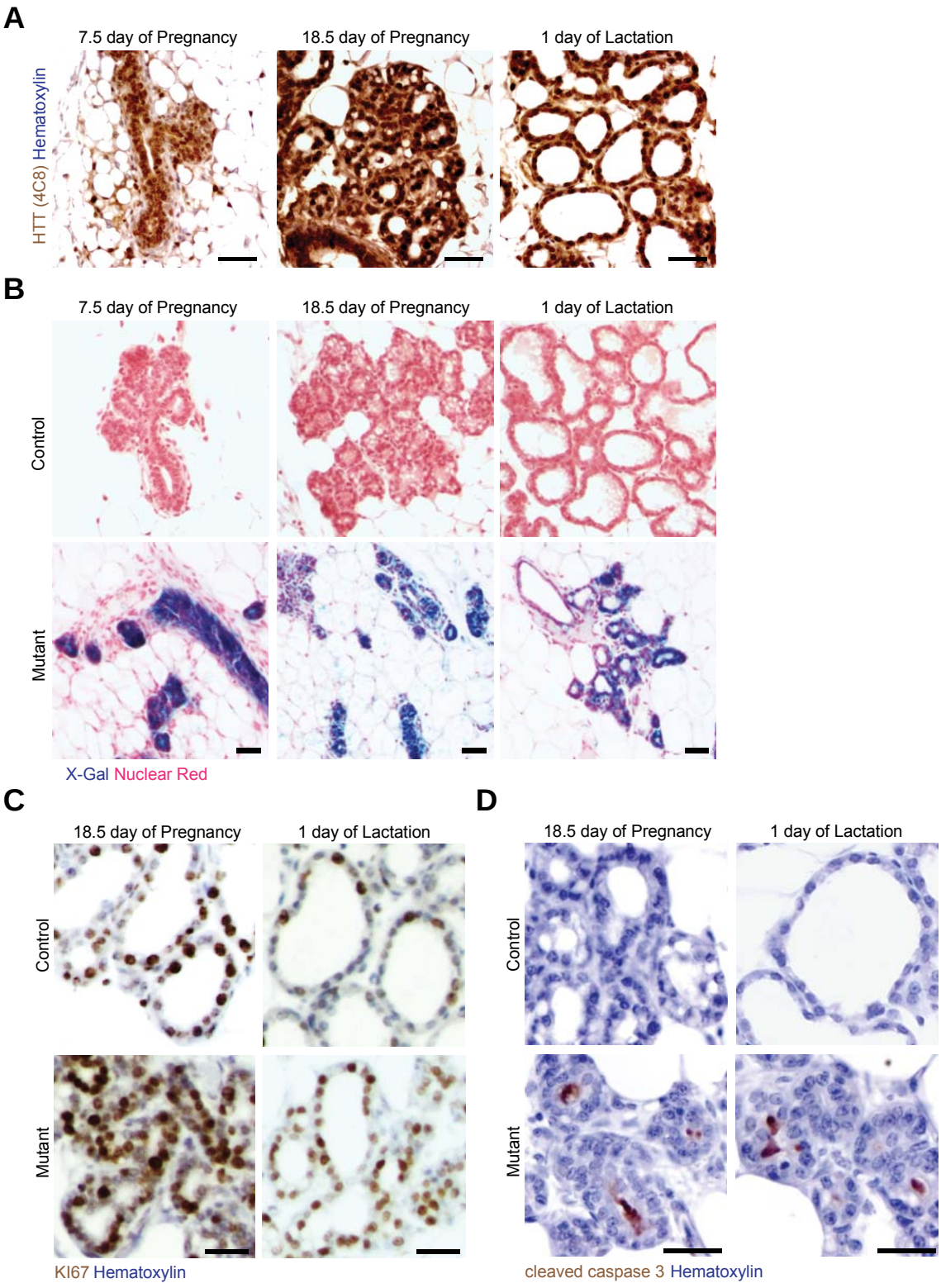
A
7.5 day of Pregnancy
18.5 day of Pregnancy
1 day of Lactation
HTT (4C8) Hematoxylin
B
7.5 day of Pregnancy
18.5 day of Pregnancy
1 day of Lactation
Control
Mutant
X-Gal Nuclear Red
C
18.5 day of Pregnancy
1 day of Lactation
Control
Mutant
KI67 Hematoxylin
D
18.5 day of Pregnancy
1 day of Lactation
Control
Mutant
cleaved caspase 3 Hematoxylin

Figure S2. Related to Figure 3

(A) Mammary gland sections from 7.5 and 18.5 day pregnant and 1 day lactating non-transgenic C57Bl6/J mice stained for HTT.

(B) Sections from *Lac-Z*-stained mammary glands derived from 7.5 and 18.5 day pregnant and 1 day lactating control and mutant K5*Cre*;*Htt*$^{flox/flox}$;*R26*.

(C) Mammary gland sections from 18.5 day pregnant and 1 day lactating control and mutant mice stained for cleaved caspase 3.

(D) Mammary gland sections from 18.5 day pregnant and 1 day lactating control and mutant mice stained for KI67.

All scale bars, 50 μm.

Figure S3

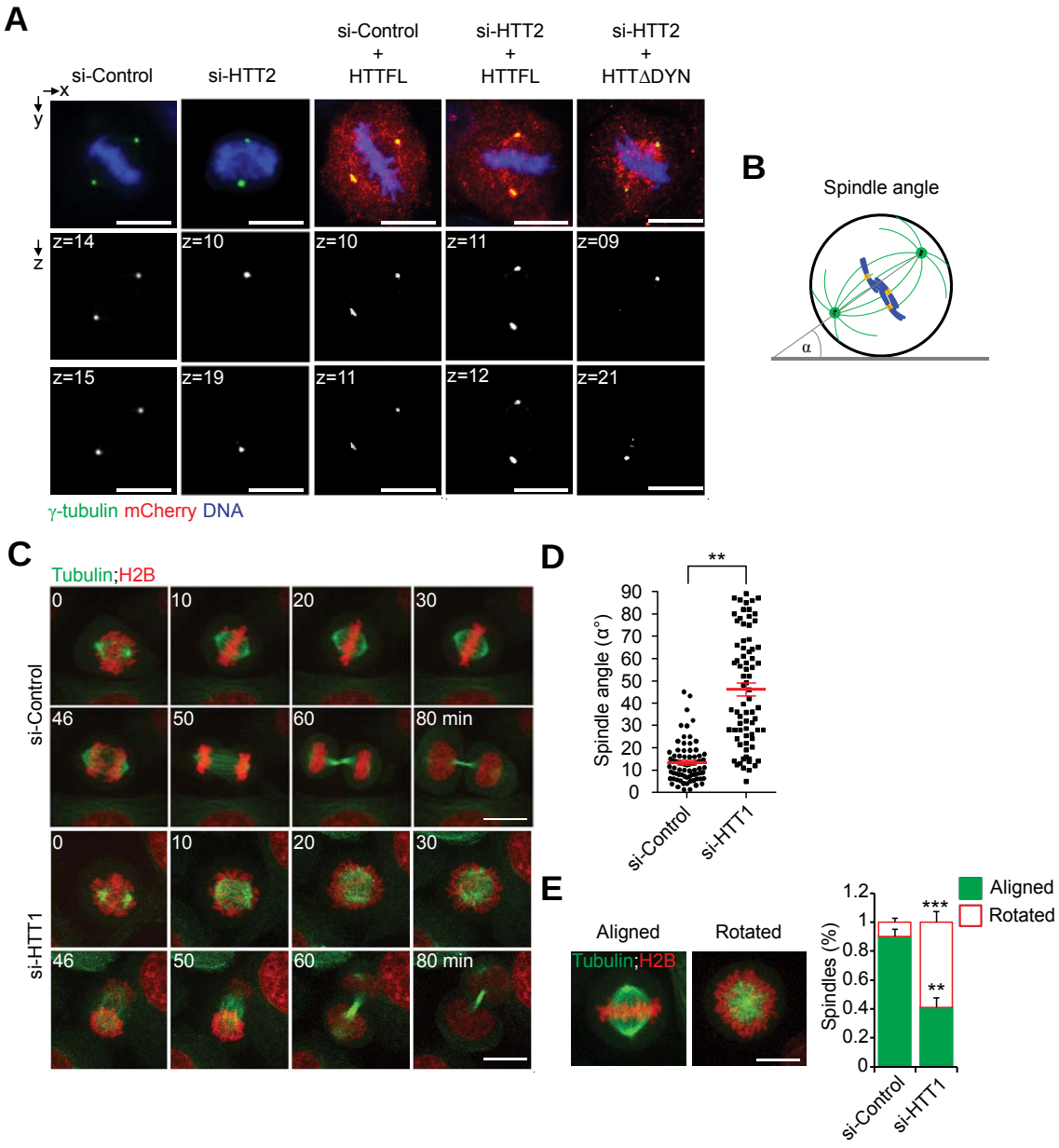

Figure S3. Related to Figure 4

(A) Mammary cells transfected with si-Control + HTTFL, si-HTT2 + HTTFL or si-HTT2 + HTTΔDYN stained for γ-tubulin (green) and HTT (mCherry, red) and counterstained with DAPI (DNA).

(B) Schemes illustrating measurement of spindle angle α in mitotic mammary cells.

(C) HeLa cells stably expressing GFP-tubulin and H2B-mCherry were transfected with si-Control or si-HTT1 RNAs and video-recorded every 2 min for 2 hr, as the cells progressed through mitosis. Image stacks of 32 planes spaced 0.6 μm apart were taken at 6 stage positions every 2 min for 2 h. Maximum intensity projections of tubulin and histone H2B are shown at the times indicated in the figure. See also Movies S1 and S2.

(D) Distribution and mean spindle angle in metaphase HeLa cells stably expressing GFP-tubulin and H2B-mCherry cells and treated with si-Control or si-HTT1 RNAs.

(E) Left: Maximum intensity projections of tubulin and histone H2B from HeLa cells stably expressing GFP-tubulin and H2B-mCherry, indicating aligned and rotated mitotic spindle during metaphase. Right: Percentage of si-Control and si-HTT1 RNA-transfected Hela cells with aligned or rotated mitotic spindle.

All scale bars, 10 μm. Error bars, SEM. ** $p<0.01$; *** $p<0.001$.

Figure S4

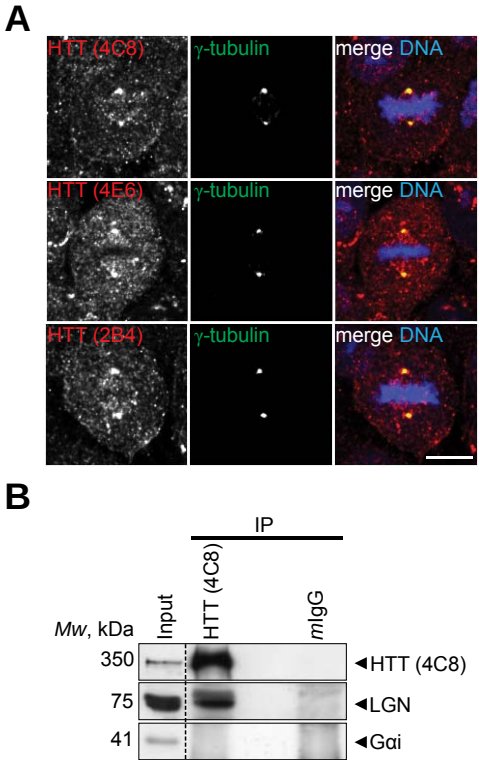

Figure S4. Related to Figure 5

(A) Mammary cells stained for γ-tubulin and HTT (4C8, 4E6 and 2B4 antibodies) and counterstained with DAPI (DNA). Scale bars, 10 µm.

(B) HTT, LGN and $G_{\alpha i}$ were immunoprecipitated using HTT (4C8) antibody from mammary cells arrested in metaphase before cell lysis. Mouse IgG (*m*IgG) was used as a negative control. The immunoprecipitates were analyzed by immunoblotting with anti-HTT (4C8), anti-LGN and anti-$G_{\alpha i}$ antibodies.

Figure S5

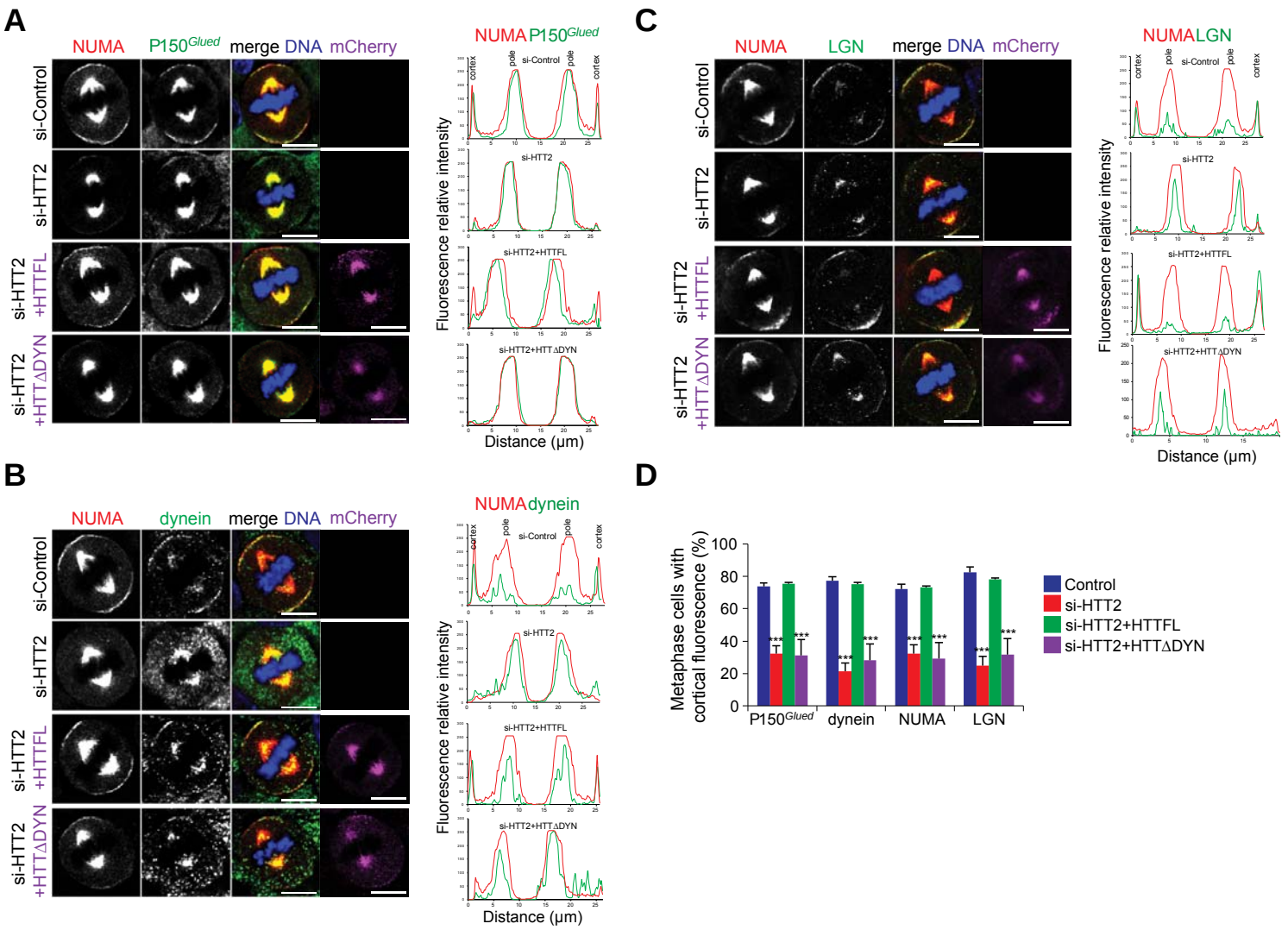

Figure S5. Related to Figure 6

(A to C) Mammary cells transfected with si-Control, si-HTT2, si-Control + HTTFL, si-HTT2 + HTTFL or si-HTT2 + HTTΔDYN and stained for NUMA and P150^{Glued} (A), dynein (B) or LGN (C) and counterstained with DAPI (DNA). Right: line scan analysis (relative fluorescence intensity) showing the spatial distribution of NUMA and P150^{Glued} (A), dynein (B) or LGN (C).

(D) Percentage of mammary cells transfected showing cortical P150^{Glued}, dynein, NUMA and LGN at metaphase.

All scale bars, 10 µm. Error bars, SEM. *** p<0.001.

Figure S6

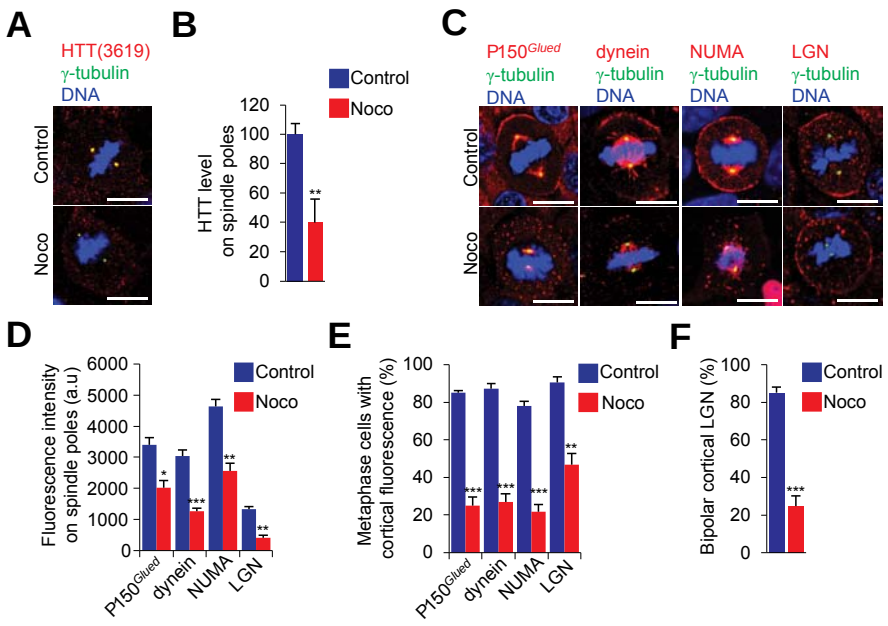

Figure S6. Related to Figure 7

(A) Mammary cells treated with DMSO (Control) or 40 nM nocodazole (Noco) for 20 min and stained for HTT and γ-tubulin and counterstained with DAPI (DNA).

(B) HTT abundance at spindle poles in Control and Noco metaphase cells.

(C) Control and Noco mammary cells stained for γ-tubulin with P150^{Glued}, dynein, NUMA or LGN and counterstained with DAPI (DNA).

(D) P150^{Glued}, dynein, NUMA and LGN abundance at spindle poles in Control and Noco mammary metaphase cells.

(E) Percentage of Control and Noco mammary cells with cortical accumulation of P150^{Glued}, dynein, NUMA and LGN at metaphase.

(F) Percentage of LGN-positive Control and Noco mammary cells with bipolar cortical LGN labelling as opposed to homogeneous labelling throughout the cell cortex.

All scale bars, 10 µm. Error bars, SEM. * $p<0.005$; ** $p<0.01$; *** $p<0.001$.

Table S1. Epithelial Markers Used

Epithelial compartment	Gene	Protein	Method
Basal	*Trp63*	P63	RT-qPCR
	Krt14	Keratin 14 (K14)	RT-qPCR, IHC
	Krt5	Keratin 5 (K5)	IHC
	Cd24	Heat stable antigen (HSA or CD24), *low expression*	FACS
	Itgb1	β1 integrin (CD29), *high expression*	IHC
	Itga6	α6 integrin (CD49F), *high expression*	FACS
	Snai1	Snail 1	RT-qPCR
	Snai2	Snail 2	RT-qPCR
	Vim	Vimentin	RT-qPCR
Luminal	*Gata3*	GATA3	RT-qPCR
	Cdh1	E-cadherin	IHC
	Krt8/18	Keratin 8/18 (K8/18)	RT-qPCR, IHC
	Cd24	Heat stable antigen (HSA or CD24), *high expression*	FACS
	Itgb1	β1 integrin (CD29), *low expression*	IHC
	Itga6	α6 integrin (CD49F), *low expression*	FACS
	Itga2	α2 integrin (CD49B), *luminal progenitors*	FACS
	Elf5	E74-like factor 5 (ELF5), *luminal progenitors*	RT-qPCR
	Kit	proto-oncogene KIT, *luminal progenitors*	RT-qPCR
	Sca1	Stem cell antigen 1 (SCA1), *mature luminal cells*	FACS
	Esr1	Estrogen receptor 1 (ER1), *mature luminal cells*	RT-qPCR, IHC
	Pgr	Progesterone receptor (PR), *mature luminal cells*	RT-qPCR
	Prlr	Prolactin Receptor (PRLR), *mature luminal cells*	RT-qPCR

Supplemental Movie Legends

Movie S1. Mitotic Spindle Positioning in Control Cells, Related to Figure S3C

HeLa cells stably expressing GFP-tubulin and mCherry-histone H2B were transfected with si-Control RNA for 72 h. Images corresponding to 32 planes spaced by 0.6 μm through the cell volume were collected every 2 min, as the cells progressed through mitosis using a spinning-disk confocal microscope (CSU-X1; Yookogawa). Maximum intensity projections of tubulin (green) and histone H2B (red) are shown through time; each frame corresponds to 2 min.

Movie S2. Loss of Huntingtin Alters Mitotic Spindle Orientation, Related to Figure S3C

HeLa cells stably expressing GFP-tubulin and mCherry-histone H2B were transfected with si-HTT1 RNA for 72 h. Images corresponding to 32 planes spaced by 0.6 μm through the cell volume were collected every 2 min, as the cells progressed through mitosis using a spinning-disk confocal microscope (CSU-X1; Yookogawa). Maximum intensity projections of tubulin (green) and histone H2B (red) are shown through time; each frame corresponds to 2 min.

Movie S3. Dynein Spatial Distribution in Control Cells, Related to Figure 6F

HeLa cells stably expressing DHC-GFP were transfected with si-HTT1 RNA for 72 h. Images corresponding to 35 planes spaced by 0.6 μm through the cell volume were collected every 3 min, as the cells progressed through mitosis using a spinning-disk confocal microscope (CSU-X1; Yookogawa). Maximum intensity projections of DHC are shown through time; each frame corresponds to 3 min.

Movie S4. Loss of Huntingtin Alters the Dynamics of Dynein, Related to Figure 6F

HeLa cells stably expressing DHC-GFP were transfected with si-HTT1 RNA for 72 h. Images corresponding to 35 planes spaced by 0.6 μm through the cell volume were collected every 3 min, as the cells progressed through mitosis using a spinning-disk confocal microscope (CSU-X1; Yookogawa). Maximum intensity projections of DHC are shown through time; each frame corresponds to 3 min.

Movie S5. LGN Spatial Distribution in Control Cells, Related to Figure 6F

HeLa cells stably expressing GFP-LGN were transfected with si-HTT1 RNA for 72 h. Images corresponding to 35 planes spaced by 0.6 μm through the cell volume were collected every 3 min, as the cells progressed through mitosis using a spinning-disk confocal microscope (CSU-X1; Yookogawa). Maximum intensity projections of LGN are shown through time; each frame corresponds to 3 min.

Movie S6. Loss of Huntingtin Alters the Dynamics of LGN, Related to Figure 6F

HeLa cells stably expressing GFP-LGN were transfected with si-HTT1 RNA for 72 h. Images corresponding to 35 planes spaced by 0.6 μm through the cell volume were collected every 3 min, as the cells progressed through mitosis using a spinning-disk confocal microscope (CSU-X1; Yookogawa). Maximum intensity projections of LGN are shown through time; each frame corresponds to 3 min.

Extended Experimental Procedures

Constructs and siRNAs

pARIS-mCherry-HTT and pARIS-mCherry-HTTΔdynein (referred to herein as HTTFL and HTTΔDYN, respectively) were previously described (Pardo et al., 2010). The RNA oligonucleotides for siRNA (Eurogentec) were annealed and used at 8 μM in MCF-10A and HeLa cells. The following pairs of oligonucleotides were used: Huhtt4487-sens (5'-GCAGGUUUUAGAUUUGCUG-3') and Huhtt4487-antisens (5'-CAGCAAAUCUAAAACCUGC-3') for siRNA against human HTT (si-HTT1); Huhtt585-sens (5'-AACUUUCAGCUACCAAGAAAG-3') and Huhtt585-antisens (5'-CUUUCUUGGUAGCUGAAAGUU-3') for siRNA against human HTT (si-HTT2) and si-dynein-sens (5'-GCAAUGCAGUGGCUCCUUU-3'), si-dynein-antisens (5'-AAAGGAGCCACUGCAUUGC-3') for siRNA against mouse/rat/human heavy chain of dynein (si-dynein) and si-kinesin-1-sens (5'-GCAGUCAGGUCAAAGAAUA-3') and si-kinesin-1-antisens (5'-UAUUCUUUGACCUGACUGC-3') for siRNA against mouse/rat/human KIF5B (si-kinesin-1). siRNA negative control (si-Control) from Eurogentec (OR-0030-neg05) was used. The HTT siRNAs were extensively used to target HTT function in dynein/dynactin dependent transport along microtubules in cells without off-target effects, as shown in rescue experiments and by the use of other siRNAs (Colin et al., 2008).

Cell lines and Transfection

MCF-10A, a spontaneously immortalized nontransformed human mammary epithelial cell line derived from the breast tissue (Soule et al., 1990) was maintained in DMEM/F12 (Invitrogen, Carlsbad, CA) supplemented with 5% donor horse serum, 20 ng/ml EGF (Peprotech, Rocky Hill,

NJ), 10 μg/ml insulin (Sigma, St Louis, MO), 1 ng/ml cholera toxin (Sigma), 100 μg/ml hydrocortisone (Sigma), 50 U/ml penicillin, and 50 μg/ml streptomycin (Invitrogen). Cells were spread in 10 cm^2 plate and in glass coverslips for immunoblotting and immunofluorescence experiments respectively, and transfected using Lipofectamin2000 (Invitrogen) with si-Control or si-HTT1/2 or si-dynein. For rescue experiments, expression of HTTFL and HTTΔDYN was achieved by co-electroporation of the HTTFL and HTTΔDYN constructs with si-Control or si-HTT2. After 48-72 hr, cells were lysed or fixed and immunoprocessed.

HeLa cells stably expressing GFP-tubulin (green) and H2B-mCherry (red) or DHC-GFP or GFP-LGN were cultured as previously described (Steigemann et al., 2009), plated on glass coverslips and transfected using Lipofectamin2000 with si-control or si-HTT1/2. After 72 hr, transfected cells were analyzed by spinning disk confocal videomicroscopy.

Drug Treatment

Drugs were dissolved in DMSO and kept at -20°C as 10 mM stock solutions. To enrich MCF-10A cells in metaphase, cells were seeded in 10 cm dishes (3 x 10^6 cells per dish) 24 h before treatment with 9 μM RO-3306 (Roche) for 18 hr allowing CDK1 inhibition (Vassilev et al., 2006). Cells were released from the G_2 block by washing three times in prewarmed drug-free media and incubated in fresh media for 35 min to enrich in metaphase cells. ~50% of cells were in metaphase (data not shown). To depolymerize astral microtubules, MCF-10A cells were treated with 40 nM nocodazole (Sigma) for 20 min.

Antibodies and Immunostaining Procedures

Anti-HTT antibodies used in this study were previously described: mAb 2B4 (epitope 49-64, clone HU 2B4, Euromedex) (Lunkes et al., 2002), mAb 4C8 (epitope 445-456, clone HU-4C8-

As, Euromedex), mAb 4E6 (epitope 1247-1646, clone HU-4E6, Millipore), pAb, SE3619 (Godin et al., 2010).

For immunofluorescence, the primary monoclonal antibodies used were: anti-α-tubulin DM1A (1:1000; Sigma), anti-NUMA (1:200; Calbiochem), anti-HTT 4C8 (1:500), anti-P150^{Glued} (1:100; BD Bioscience), anti-intermediary chain 74.1 of mammalian cytoplasmic dynein (1:200; Chemicon), anti-γ-tubulin GTU88 (1:300; Sigma) and anti-heavy chain KIF5A/B of mammalian cytoplasmic kinesin-1 (1:200; Covance). The primary polyclonal antibodies used were: anti-HTT SE3619 (1:100), anti-NUMA (1:200; Novus Biologicals), anti-LGN (Kaushik et al., 2003) and anti-γ-tubulin AT15 (1:500; Sigma). Secondary antibodies used were goat anti-mouse and anti-rabbit conjugated to AlexaFluor-488 or AlexaFluor-555 (Molecular Probes) at 1:200. Cells were grown on glass coverslip transfected with various constructs or siRNA.

To analyze HTT localization during mitosis, cells were prelysed 30 sec in prewarmed 0.5% Triton X-100-PHEM buffer before being fixed in anhydrous methanol at -20°C for 3 min and incubated with anti-HTT 4C8, anti-HTT 2B4, anti-HTT 4E6 or anti-HTT SE3619 and γ-tubulin. Alternatively, cells were fixed in anhydrous methanol at -20°C, containing 2% paraformaldehyde for 2 min and incubated with anti-HTT 4C8 or anti-HTT SE3619 and anti-P150^{Glued}, anti-dynein, anti-NUMA or anti-LGN overnight at 4°C.

P150^{Glued}, dynein, NUMA and LGN at spindle poles and the cell cortex were visualized as follow: cells were first fixed with 10% trichloacetic acid for 7 min. Then cells were fixed for 10 min in cold methanol (-20°C) and washed 3 times before immunostaining. Cells were double immunostained with anti-NUMA and anti-P150^{Glued} or anti-dynein or anti-LGN antibodies overnight at 4°C and then with anti-mouse and anti-rabbit AlexaFluor-488 or AlexaFluor-555.

For all immunostainings, the slides were counterstained with DAPI (Roche) and mounted in Mowiol. The pictures were captured either with a three-dimensional deconvolution imaging system or with a Leica SP5 laser scanning confocal microscope equipped with a X63 oil-immersion objective. *Z*-stack steps were of 0.2 μm. Images were treated with ImageJ (http://rsb.info.nih.gov/ij/, NIH, USA).

Spindle Orientation Quantification and Image Analyses

For quantification of HTT, HTTFL, HTTΔYN, P150^{Glued}, NUMA, LGN or kinesin-1 at spindle poles, cells were stained for the protein of interest and γ-tubulin. Quantification was achieved using 3D object counter plug-in (Bolte and Cordelieres, 2006); available at http://imagejdocu.tudor.lu/doku.php?id=plugin:analysis:3d_object_counter:start. Total volume and intensity of the particles were retrieved for further analysis.

To measure the relative fluorescence intensity of NUMA, P150^{Glued}, dynein and LGN, at spindle poles and the cell cortex, a 30-pixel line was drawn across the spindle poles and the opposing cell borders using ImageJ software. The Line Scan function of ImageJ was used to reveal the relative fluorescence intensity across the line.

Spindle orientation in MCF-10A metaphase cells was quantified using ImageJ software (http://rsb.info.nih.gov/ij/, NIH, USA). A line crossing both spindle poles was drawn on the *Z* projection pictures and repositioned along the *Z*-axis using the stack of *Z*-sections. The angle between the pole-pole and the substratum plane was calculated by an ImageJ Plug-in (Godin et al., 2010). Spindle lengths and cell lengths were quantified along the line that crosses both spindle poles.

Live-Cell Microscopy

For live-cell imaging, cells were plated in 24 mm coverglass, mounted in 6-well plate (TPP). Imaging was performed at 37°C in 5% CO_2 using an inverted microscope (Eclipse T*i*; Nikon) with a 60 x 1.42 NA oil immersion objective coupled to a spinning-disk confocal system (CSU-X1; Yookogawa) fitted with an EM-CCD camera (Evolve; Photometrics). Exposure times were 50 msec for GFP-tubulin or mCherry-tagged histone H2B and 10% laser power, 200 msec and 8% laser power for GFP-LGN, and 200 msec and 15% laser power for DHC-GFP. For Figure 5G, image stacks of 32 planes spaced 0.6 μm apart were taken at 6 stage positions every 2 min for 2 h. For Figure 7F, 35 planes spaced 0.6 μm apart were captured at 10 stage positions every 3 min for 2 h. Maximum intensity projection of the fluorescent channels was performed. Images were treated with ImageJ.

Cell Extracts, Immunoblotting and Immunoprecipitation Experiments

MCF-10A and Hela cells were lysed in NP40 buffer (50 mM Tris, pH 7.4, 250 mM NaCl, 5 mM EDTA, 50 mM NaF, 1 mM Na3VO4, 1% Nonidet P40 (NP40), 0.02% NaN_3), containing protease inhibitor cocktail (Sigma), and centrifuged at 11,000 x g for 10 min at 4°C. Proteins (20-30 μg) were loaded onto SDS-PAGE (polyacrylamide gel electrophoresis) and subjected to Western blot analysis. Primary monoclonal antibodies used were: anti-HTT 4C8 (1:3000), anti-$P150^{Glued}$ (1:1000), anti-α-tubulin (1:5000), anti-dynein (1:1000) and anti-kinesin-1 (1:1000). Primary polyclonal antibodies used were: anti-NUMA (1:1000), anti-LGN (1:500), anti-$G_{\alpha i1}$ (1:1000; Santa Cruz Biotechnology) and anti-mCherry (1:1000; Institut Curie, Paris). Secondary HRP-conjugated goat anti-mouse/anti-rabbit antibodies (Amersham) at 1:10 000 were used.

For immunoprecipitations, metaphase MCF-10A cells were lysed in IP buffer (Tris 50 mM, pH 7.4, 250 mM NaCl, 5 mM EDTA, 50 mM NaF, 1% Na_3VO_4, 1% NP40, 0.02% NaN_3, 50mM KH_2PO_4) containing protease inhibitor cocktail. Lysates (500 µg at 1 µg/µl) were precleared 1 h at 4°C with 50 µl of a 50% solution of protein A or G beads. Extracts were incubated for 1 h at 4°C with 5 µg of anti-HTT (4C8) antibody or anti-dynein or anti-IgG prebound with 50 µl of a 50% solution of protein A or G sepharose beads (Sigma). Beads were washed three times with IP buffer. Bound proteins were eluted with SDS loading buffer and resolved by SDS-PAGE and subjected to immunoblotting analysis.

Mouse Strains

Transgenic mice expressing the Rosa26LacZ reporter strain, carrying a loxP-stop loxP-lacZ cassette, and the Cre recombinase under the control of the K5 promoter (K5*Cre*) were provided by P. Soriano and J. Jorcano (Ramirez et al., 2004; Soriano, 1999). The generation of $Htt^{flox/flox}$ mice was previously described (Dragatsis et al., 2000). All mice were bred in a 129SV/C57BL6 genetic background. $Htt^{flox/flox}$ mice were used as controls and K5*Cre*;$Htt^{flox/flox}$ as mutants. All experiments were performed in strict accordance with the recommendations of the European Community (86/609/EEC) and the French National Committee (87/848) for care and use of laboratory animals (permissions 91-448 to S.H. and 76-102 to S.E.).

Whole Mounts

Whole mounts were prepared by fixing the glands on glass slides with MethaCarn solution (60% methanol, 30% chloroform, 10% glacial acetic acid) overnight at room temperature. The mounts were hydrated by sequential incubation in ethanol solutions of decreasing concentration: 100%, (overnight), 70%, 50%, and 30% (15 min each), distilled water (2 x 5 min), and stained overnight

with an aqueous solution of 2% carmine (Sigma, Buchs, Switzerland) and 5% aluminum potassium sulphate (Sigma, Buchs, Switzerland). The mounts were dehydrated in ethanol solutions (70%, 90%, 95%, and 2 x 100%, for 15 min each) and cleared with xylene overnight. Images were captured with an Epson Perfection 3200 scanner.

X-Gal Staining

For whole-mount X-Gal staining, mammary glands were fixed in 2.5% paraformaldehyde in PBS, pH 7.5, for 1 hr at 4°C, and stained overnight at 30°C (Biology of the Mammary Gland, http://mammary.nih.gov). For histological analyses, glands were embedded in paraffin, and 7 µm-thick sections were cut, dewaxed and counterstained with Nuclear Fast Red.

Histology and Immunostaining

Dissected mammary fat pads were spread out on a glass slide, fixed in MethaCarn and embedded in paraffin. 7 µm-thick Sections were cut and deparaffinized before staining. Sections were incubated overnight at 4 °C with primary antibodies, followed by incubation for 1 hr at room temperature with secondary antibodies and 3 min with DAPI. Primary antibodies used were: rabbit polyclonal anti-K5 (1:2000; Covance), anti-K14 (1:500; clone AF64, Covance), anti-PAR3 (1:200; Chemicon), anti-aPKC (1:200; clone C-20, Santa Cruz Biotechnology), anti-p-STAT5A (Tyr694, 1:100; Cell Signalling), anti-cleaved caspase 3 (1:100; Cell Signalling), anti-WAP (1:300; clone R-131; Santa Cruz Biotechnology), anti-ERα (1:50; Santa Cruz Biotechnology); rabbit monoclonal anti-KI67 (1:100; clone SP6, Neo Markers); rat monoclonal anti-β1 integrin (1:200; clone MB1.2, Chemicon) and mouse monoclonal anti K8 (1:100; clone Ks 8.7, Progen Biotechnik), anti-α-smooth muscle actin (1:100; clone 1A4, Sigma-Aldrich), anti-α-tubulin

DM1A (1:1000; Sigma), anti-ZO1 (1:50; Invitrogen), anti-E-cadherin (1:200; BD Bioscience). Antigen retrieval was performed by boiling the slides for 10 min in a microwave in 10 mM citrate buffer (pH 6) for cleaved caspase 3, KI67 and p-STAT5A, or in EDTA buffer (pH 8.8) for 10 min for PAR3, aPKC, ZO1 and E-cadherin antibodies. Secondary antibodies used were goat anti-mouse and anti-rabbit conjugated to AlexaFluor-488 or AlexaFluor-555 or Biotin (Vector Laboratories).

Alternatively, frozen 10 to 14 μm-thick sections were cut and air-dried for 30 min, then fixed for 10 min with 4% paraformaldehyde, demasked with acetone at -20°C, for 10 min for γ-tubulin staining, and then blocked for 1 h in BSA/NGS block (3% BSA, 5% NGS, 0.2% Triton X-100 in PBS). Sections were incubated overnight at 4 °C with primary antibodies, followed by incubation for 1 h at room temperature with secondary antibodies and 3 min with DAPI. Primary antibodies used were: rabbit polyclonal anti-NUMA (1:100), anti-LGN (1:100), anti-K5 (1:500); rat monoclonal anti-β1 integrin (1:200; clone MB 1.2, Chemicon); mouse monoclonal anti-HTT (4C8, 1:300), anti-α-tubulin (1:500) and anti-γ-tubulin (1:200). Secondary antibodies used were goat anti-mouse, anti-rat and anti-rabbit conjugated to AlexaFluor-488 or AlexaFluor-555 or AlexaFluor-647 (Vector Laboratories).

Ventral skin of E18 embryos was fixed in 4% paraformaldehyde and immunostained as described elsewhere (Kogata and Howard, 2013). Primary antibodies used were: rabbit polyclonal anti-K5 (1:200; Covance); anti-β-glactosidase (1:100; 5 Prime 3 Prime) and mouse monoclonal anti K8 (1:50; clone Ks 8.7, Progen Biotechnik). Secondary antibodies used were goat anti-mouse and anti-rabbit conjugated to AlexaFluor-488 or AlexaFluor-555 (Vector Laboratories).

Isolation of the Mammary Epithelial Cells and Flow Cytometry

To isolate mammary epithelial cells, mammary fat pads were mechanically dissociated with scissors and scalpel and digested for 90 min at 37 °C in CO2-independent medium (Invitrogen) supplemented with 5% fetal bovine serum, 3 mg/ml collagenase (Roche Diagnostics) and 100 U/ml hyaluronidase (Sigma). Cells were sequentially resuspended in 0.25% trypsin-EDTA for 1 min, and then 5 min in 5 mg/ml dispase (Roche Diagnostics) with 0.1 mg/ml DNase I (Sigma) followed by filtration trough a 40-μm mesh. Red blood cells were lysed in NH_4Cl.

To separate basal and luminal cells, mammary epithelial cells isolated from the inguinal glands of five 12-week-old virgin K5*Cre* mice were pooled, stained with anti-CD24-FITC (clone M1/69; BD Pharmingen), anti-CD49F-PE (clone OXM178; Chemicon), anti-CD45-APC (clone 30-F11; Biolegend) and anti-CD31-APC (clone MEC13.3; Biolegend) antibodies, as described elsewhere (Shackleton et al., 2006; Stingl et al., 2006; Taddei et al., 2008). CD24-low/α6-high (basal) and CD24-high/α6-low (luminal) cells were purified using FACSAria III (SORP) (Becton Dickinson). CD45- and CD31-positive stromal cells were excluded from the flow cytometry analysis. Conjugated isotype-matching IgGs were used as negative controls.

To separate different sub-populations within luminal compartment, sorted luminal cells (pure at 98%) were stained with anti-CD49B-APC (clone HMα2, BD Pharmingen) and anti-SCA1-PE-Cy7 (clone D7, BD Pharmingen) antibodies. The following cell populations were purified: $SCA1^+/CD49B^-$, $SCA1^+/CD49B^+$ and $SCA1^-/CD49B^+$ (Shehata et al., 2012).

Mammary Colony Forming Assay

In vitro Matrigel colony forming assays were performed as described (Stingl et al., 2006). Single mammary cell suspensions were prepared from the inguinal glands and 5,000 BCs or LCs were

seeded in 50 µL Matrigel and cultured in DMEM/F12 medium containing 1% fetal calf serum (FCS), B27. Colonies were scored after 6 days.

Quantitative RT-PCR

RNA samples were retrotranscribed using the First-Strand cDNA Synthesis Kit (Invitrogen). cDNAs were diluted 1:10 and submitted to RT-PCR with 7900HT Fast real time PCR system (Applied biosystems) using power SYBR Green PCR Master mix (Applied biosystems) with the following oligonucleotide pairs: *Htt* (5'-CTCAGAAGTGCAGGCCTTACCT-3', 5'-GATTCCTCCGGTCTTTTGCTT-3' and 5'-CTCAGAAGTGCAGGCCTTACCT-3', 5'-GATTCCTCCGGTCTTTTGCTT-3') (Benn et al., 2008), *Cre* (5'-TTCCCGCAGAACCTGAAGAT-3', 5'- GCCGCATAACCAGTGAAACA-3') (Taddei et al., 2008), *Gata3* (5'- AGCCACATCTCTCCCTTCAG-3', 5'-AGGGCTCTGCCTCTCTAACC-3'), *Dll1* (5'-CATGAACAACCTAGCCAATTGC-3', 5'-GCCCCAATGATGCTAACAGAA-3'), *Dll3* (5'-CCTGAGGTTACAAGACGGTGCT-3', 5'-CAGGCCTCTCGTGCATAAATG-3'), *Jag1* (5'-ACACAGGGATTGCCCACTTC-3', 5'-AGCCAAAGCCATAGTAGTGGTCAT-3'), *Jag2* (5'-CGACTCACACTGCGCTTCA-3', 5'-TCGGATTCCAGAGCAGATAGC-3'), *Notch1* (5'-ACAACAACGAGTGTGAGTCC-3', 5'-ACACGTGGCTCCTGTATATG-3'), *Notch2* (5'-TGACTGTTCCCTCACTATGG-3', 5'-CACGTCTTGCTATTCCTCTG-3'), *Notch3* (5'-AGATCAATGAGTGTGCATCC-3', 5'-GCAGACTCCATGACTACAGG-3'), *Notch4* (5'-GAGGACCTGGTTGAAGAATTGATC-3', 5'-TGCAGTTTTTCCCCTTTTATCC-3'), *Hey1* (5'-TGAGCTGAGAAGGCTGGTAC-3', 5'-ACCCCAAACTCCGATAGTCC-3'), *Hes6* (5'-AAGCTAGAGAACGAAGAGGT-3', 5'-TCAGCTGAGAAGTGGCATC-3') (Bouras et al., 2008), *Krt14* (5'-GCTCTTGTGGTATCGGTGGT-3', 5'-GAGGAGAAGCGAGAGGAGGT-3'), *Krt18* (5'-CGAGGCACTCAAGGAAGAAC-3', 5'-AATCTGGGCTTCCAGACCTT-3') , *Trp63*

(5’-AGCAGCACCAGCACCTACTT-3’, 5’-ATTCCTGAAGCAGGCTGAAA-3’), *Kit* (5’-AGTGCTTCCGTGACATTCAAC-3’, 5’-TGCCATTTATGAGCCTGTCGT-3’), *Elf5* (5’-CCAACGCATCCTTCTGTGAC-3’, 5’-AGGCAGGGTAGTAGTCTTCA-3’), *Esr1* (5’-CTGGACAGGAATCAAGGTAAA-3’, 5’-GAGGCACACAAACTCTTCTC-3’), *Pgr* (5’-CCACCTGTACTGCTTGAATAC-3’, 5’-CAACTGGGCAGCAATAACTTC-3’), *Prlr* (5’-ATAAAAGGATTTGATACTCATCTG-3’, 5’-GTCATCCACTTCCAAGAACTC-3’), *Snai1* (5’-ACACCTGTTTCACAGCAGTT-3’, 5’- TAGTTCTGGGAGACACATTG - 3’), *Snai2* (5’-GATGCCCAGTCTAGGAAATC-3’, 5’-CCCAGTGTGAGTTCTAATGT-3’), *Vim* (5’-CCAAGCAGGAGTCAAACGA-3’, 5’-TAAGGGCATCCACTTCACAG-3’), *Ki67* (5’-TCAATGTGCCTCGCAGTAAG-3’, 5’-GCATCTTTGGGGTTTTCTCA-3’), *Wap* (5’-AACATTGGTGTTCCGAAAGC-3’, 5’-GGTCGCTGGAGCATTCTATC-3’), *Csn2* (5’-TGCAGGCAGAGGATGTGCTCCAGGCT-3’, 5’-GGCCTGGGGCTGTGACTGGATGCT-3’) (Primer3v.0.4.0; http://bioinfo.ut.ee/primer3-0.4.0/primer3). *β-actin* (5’-AGGTGACAGCATTGCTTCTG-3’, 5’-GCTGCCTCAACACCTCAAC-3’) and *hprt* (5’-GCTGGTGAAAAGGACCTCT-3’, 5’-CACAGGACTAGAACACCTGC-3’) (Moreira Sousa et al., 2013) genes were used as internal controls. Fold changes were calculated using the ddCT method.

Statistical Analyses

Figure 1B
Data are from four independent cell sorting experiments: 5 mice per experiment
T test **p<0.01
Figure 1D
Data are from four independent cell sorting experiments: control: 5 mice per experiment, mutant: 5 mice per experiment
T test *p<0.05; **p<0.01
Figure 1F
Data are from four independent cell sorting experiments: control: 5 mice per experiment, mutant: 5 mice per experiment
T test **p<0.01; ***p<0.001
Figure 1G
Data are from four independent cell sorting experiments: control: 5 mice per experiment, mutant: 5 mice per experiment
T test *p<0.05
Figure 1H
Data are from four independent cell sorting experiments: control: 5 mice per experiment, mutant: 5 mice per experiment
T test ***p<0.001
Figure 1I
Data are from four independent cell sorting experiments: control: 5 mice per experiment, mutant: 5 mice per experiment
T test ***p<0.001

Figure 2A
Data are from four independent cell sorting experiments: control: 5 mice per experiment, mutant: 5 mice per experiment
T test *p<0.05; **p<0.01; ***p<0.001
Figure 2B
Data are from four independent cell sorting experiments: control: 5 mice per experiment, mutant: 5 mice per experiment
T test *p<0.05; **p<0.01; ***p<0.001
Figure 2D
Data are from: control: 4 mice; mutant: 4 mice
T test ***p<0.001
Figure 2E
Data are from: control: 4 mice; mutant: 4 mice
T test ***p<0.001
Figure 2G
Data are from three independent cell sorting experiments: control: 5 mice per experiment, mutant: 5 mice per experiment
T test *p<0.05; ***p<0.001
Figure 2H
Data are from three independent cell sorting experiments: control: 5 mice per experiment, mutant: 5 mice per experiment

T test ***p<0.001

Figure 3A
Data are from: control: 8 mice; mutant: 6 mice
T test *p<0.05
Figure 3B
Data are from: control: 5 mice; mutant: 5 mice
T test **p<0.01
Figure 3C
Data are from: control: 5 mice; mutant: 5 mice
T test ***p<0.01
Figure 3D
Data are from control: 3 mice; mutant: 3 mice
T test ***p<0.001

Figure 4D
Data are from: control: 10 mice (68 cells), mutant: 9 mice (62 cells)
T test ***p<0.001
Figure 4E
Data are from: control: 10 mice (43 cells), mutant: 9 mice (38 cells)
T test ***p<0.001
Figure 4F
Metaphase: Data are from: control: 10 mice (68 cells), mutant: 9 mice (62 cells)
Telophase: Data are from: control: 10 mice (43 cells), mutant: 9 mice (38 cells)
T test **p<0.01; ***p<0.001
Figure 4H
Data are from three independent experiments: si-Control: 64 cells, si-HTT1: 59 cells, si-dynein: 43 cells
ANOVA F[2,163] =7.018; p***<0.001
Fisher's PLSD:

	p-value
si-Control, si-HTT1	<0.001
si-Control, si-dynein	<0.001
si-HTT1, si-dynein	0.2488

Figure 4I
Data are from three independent experiments: si-Control: 98 cells, si-HTT1: 72 cells, si-dynein: 52 cells
ANOVA F[2,219] =37.60; p***<0.0001
Fisher's PLSD:

	p-value
si-Control, si-HTT1	<0.0001
si-Control, si-dynein	<0.0001
si-HTT1, si-dynein	0.2393

Figure 4K
Data are from five independent experiments: si-Control: 35 cells, si-HTT2: 32 cells, si-Control+HTTFL: 31 cells, si-HTT2+HTTFL: 30 cells, si-HTT2+HTTΔDYN: 32 cells

ANOVA F[4,155] =23.90; p***<0.0001
Fisher's PLSD:

	p-value
si-Control, si-HTT2	<0.0001
si-Control, si-Control+HTTFL	0.4907
si-Control, si-HTT2+HTTFL	0.5626
si-Control, si-HTT2+HTTΔDYN	<0.0001
si-HTT2, si-Control+HTTFL	<0.0001
si-HTT2, si-HTT2+HTTFL	<0.001
si-HTT2, si-HTT2+HTTΔDYN	0.2887
si-Control+HTTFL, si-HTT2+HTTFL	0.2177
si-Control+HTTFL, si-HTT2+HTTΔDYN	<0.0001
si-HTT2+HTTFL, si-HTT2+HTTΔDYN	<0.0001

Figure 4L
Data are from five independent experiments: si-Control+HTTFL: 34 cells, si-HTT2+HTTFL: 32 cells, si-HTT2+HTTΔDYN: 30 cells
ANOVA F[2,93] =11.80; p***<0.0001
Fisher's PLSD:

	p-value
si-Control+HTTFL, si-HTT2+HTTFL	0.3182
si-Control+HTTFL, si-HTT2+HTTΔDYN	<0.001
si-HTT2+HTTFL, si-HTT2+HTTΔDYN	<0.001

Figure 6D
Data are from three independent experiments:
Dynein: si-Control: 51 cells, si-HTT1: 53 cells
P150^{Glued}: si-Control: 36 cells, si-HTT1: 33 cells
NUMA: si-Control: 62 cells, si-HTT1: 57 cells
LGN: si-Control: 54 cells, si-HTT1: 40 cells
T test ***p<0.001
Figure 6G
Data are from three independent experiments: si-Control: 105 DHC-GFP cells and 88 LGN-GFP cells, si-HTT1: 92 DHC-GFP cells and 73 GFP-LGN cells
T test ***p<0.001

Figure 7D
Data are from three independent experiments: si-Control: 37 cells, si-HTT1: 39 cells
T test ***p<0.001
Figure 7E
Data are from three independent experiments: si-Control: 37 cells, si-HTT1: 39 cells
T test ***p<0.001
Figure 7H
Data are from three independent experiments:
P150^{Glued}: si-Control: 40 cells, si-kinesin-1: 40 cells
Dynein : si-Control: 39 cells, si-kinesin-1: 36 cells
NUMA: si-Control: 49 cells, si-kinesin-1: 52 cells

T test ***p<0.001

Figure 7I

Data are from three independent experiments: si-Control: 30 cells, si-kinesin-1: 33 cells
T test **p<0.01

Figures S1B and S1C

Data are from three independent cell sorting experiments: control: 5 mice per experiment, mutant: 5 mice per experiment
T test ***p<0.001

Figure S3D

Data are from three independent experiments: si-Control: 77 cells, si-HTT1: 75 cells
T test **p<0.01

Figure S3E

Data are from three independent experiments: si-Control: 108 cells, si-HTT1: 100 cells
T test **p<0.01; ***p<0.001

Figure S5D

P150^{Glued}: Data are from three independent experiments: si-Control: 32 cells, si-HTT2: 30 cells, si-HTT2+HTTFL: 30 cells, si-HTT2+HTTΔDYN: 30 cells
ANOVA F[3,8] =281.3; p***<0.0001
Fisher's PLSD:

	p-value
si-Control, si-HTT2	<0.0001
si-Control, si-HTT2+HTTFL	0.4892
si-Control, si-HTT2+HTTΔDYN	<0.0001
si-HTT2, si-HTT2+HTTFL	<0.0001
si-HTT2, si-HTT2+HTTΔDYN	0.2564
si-HTT2+HTTFL, si-HTT2+HTTΔDYN	<0.0001

Dynein: Data are from three independent experiments: si-Control: 34 cells, si-HTT2: 29 cells, si-HTT2+HTTFL: 30 cells, si-HTT2+HTTΔDYN: 30 cells
ANOVA F[3,8] =81.7; p***<0.0001
Fisher's PLSD:

	p-value
si-Control, si-HTT2	<0.0001
si-Control, si-HTT2+HTTFL	0.3492
si-Control, si-HTT2+HTTΔDYN	<0.0001
si-HTT2, si-HTT2+HTTFL	<0.0001
si-HTT2, si-HTT2+HTTΔDYN	0.1659
si-HTT2+HTTFL, si-HTT2+HTTΔDYN	<0.0001

NUMA: Data are from three independent experiments: si-Control: 37 cells, si-HTT2: 33 cells, si-HTT2+HTTFL: 33 cells, si-HTT2+HTTΔDYN: 31 cells
ANOVA F[3,8] =89.8; p***<0.0001
Fisher's PLSD:

	p-value
si-Control, si-HTT2	<0.0001

si-Control, si-HTT2+HTTFL	0.3377
si-Control, si-HTT2+HTTΔDYN	<0.0001
si-HTT2, si-HTT2+HTTFL	<0.0001
si-HTT2, si-HTT2+HTTΔDYN	0.4247
si-HTT2+HTTFL, si-HTT2+HTTΔDYN	<0.0001

LGN: Data are from three independent experiments: si-Control: 33 cells, si-HTT2: 33 cells, si-HTT2+HTTFL: 30 cells, si-HTT2+HTTΔDYN: 30 cells
ANOVA F[3,8] =158.7; p***<0.0001
Fisher's PLSD:

	p-value
si-Control, si-HTT2	<0.0001
si-Control, si-HTT2+HTTFL	0.1111
si-Control, si-HTT2+HTTΔDYN	<0.0001
si-HTT2, si-HTT2+HTTFL	<0.0001
si-HTT2, si-HTT2+HTTΔDYN	0.6054
si-HTT2+HTTFL, si-HTT2+HTTΔDYN	<0.0001

Figure S6B
Data are from three independent experiments: Control: 32 cells, Noco: 37 cells
T test **p<0.01

Figure S6D
Data are from three independent experiments:
P150^{Glued}: Control: 53 cells, Noco: 62 cells
Dynein: Control: 35 cells, Noco: 32 cells
NUMA: Control: 61 cells, Noco: 58 cells
LGN: Control: 51 cells, Noco: 45 cells
T test *p<0.05; **p<0.01; ***p<0.001

Figure S6E
Data are from three independent experiments:
P150^{Glued}: Control: 53 cells, Noco: 62 cells
Dynein: Control: 35 cells, Noco: 32 cells
NUMA: Control: 61 cells, Noco: 58 cells
LGN: Control: 51 cells, Noco: 45 cells
T test **p<0.01; ***p<0.001

Figure S6F
Data are from three independent experiments: Control: 61 cells, Noco: 45 cells
T test ***p<0.001

Supplemental References

Benn, C.L., Fox, H., and Bates, G.P. (2008). Optimisation of region-specific reference gene selection and relative gene expression analysis methods for pre-clinical trials of Huntington's disease. Mol Neurodegener *3*, 17.

Bolte, S., and Cordelieres, F.P. (2006). A guided tour into subcellular colocalization analysis in light microscopy. J Microsc *224*, 213-232.

Bouras, T., Pal, B., Vaillant, F., Harburg, G., Asselin-Labat, M.L., Oakes, S.R., Lindeman, G.J., and Visvader, J.E. (2008). Notch signaling regulates mammary stem cell function and luminal cell-fate commitment. Cell Stem Cell *3*, 429-441.

Dragatsis, I., Levine, M.S., and Zeitlin, S. (2000). Inactivation of Hdh in the brain and testis results in progressive neurodegeneration and sterility in mice. Nat Genet *26*, 300-306.

Godin, J.D., Colombo, K., Molina-Calavita, M., Keryer, G., Zala, D., Charrin, B.C., Dietrich, P., Volvert, M.L., Guillemot, F., Dragatsis, I.*, et al.* (2010). Huntingtin is required for mitotic spindle orientation and mammalian neurogenesis. Neuron *67*, 392-406.

Kaushik, R., Yu, F., Chia, W., Yang, X., and Bahri, S. (2003). Subcellular localization of LGN during mitosis: evidence for its cortical localization in mitotic cell culture systems and its requirement for normal cell cycle progression. Mol Biol Cell *14*, 3144-3155.

Kogata, N., and Howard, B.A. (2013). A whole-mount immunofluorescence protocol for three-dimensional imaging of the embryonic mammary primordium. J Mammary Gland Biol Neoplasia *18*, 227-231.

Lunkes, A., Lindenberg, K.S., Ben-Haiem, L., Weber, C., Devys, D., Landwehrmeyer, G.B., Mandel, J.L., and Trottier, Y. (2002). Proteases acting on mutant huntingtin generate cleaved products that differentially build up cytoplasmic and nuclear inclusions. Mol Cell *10*, 259-269.

Moreira Sousa, C., McGuire, J.R., Thion, M.S., Gentien, D., de la Grange, P., Tezenas du Montcel, S., Vincent-Salomon, A., Durr, A., and Humbert, S. (2013). The Huntington disease protein accelerates breast tumour development and metastasis through ErbB2/HER2 signalling. EMBO Mol Med *5*, 309-325.

Pardo, R., Molina-Calavita, M., Poizat, G., Keryer, G., Humbert, S., and Saudou, F. (2010). pARIS-htt: an optimised expression platform to study huntingtin reveals functional domains required for vesicular trafficking. Mol Brain *3*, 17.

Ramirez, A., Page, A., Gandarillas, A., Zanet, J., Pibre, S., Vidal, M., Tusell, L., Genesca, A., Whitaker, D.A., Melton, D.W.*, et al.* (2004). A keratin K5Cre transgenic line appropriate for tissue-specific or generalized Cre-mediated recombination. Genesis *39*, 52-57.

Soriano, P. (1999). Generalized lacZ expression with the ROSA26 Cre reporter strain. Nat Genet *21*, 70-71.

Soule, H.D., Maloney, T.M., Wolman, S.R., Peterson, W.D., Jr., Brenz, R., McGrath, C.M., Russo, J., Pauley, R.J., Jones, R.F., and Brooks, S.C. (1990). Isolation and characterization of a spontaneously immortalized human breast epithelial cell line, MCF-10. Cancer Res *50*, 6075-6086.

Steigemann, P., Wurzenberger, C., Schmitz, M.H., Held, M., Guizetti, J., Maar, S., and Gerlich, D.W. (2009). Aurora B-mediated abscission checkpoint protects against tetraploidization. Cell *136*, 473-484.

Stingl, J., Eirew, P., Ricketson, I., Shackleton, M., Vaillant, F., Choi, D., Li, H.I., and Eaves, C.J. (2006). Purification and unique properties of mammary epithelial stem cells. Nature *439*, 993-997.

Taddei, I., Deugnier, M.A., Faraldo, M.M., Petit, V., Bouvard, D., Medina, D., Fassler, R., Thiery, J.P., and Glukhova, M.A. (2008). Beta1 integrin deletion from the basal compartment of the mammary epithelium affects stem cells. Nat Cell Biol *10*, 716-722.

Vassilev, L.T., Tovar, C., Chen, S., Knezevic, D., Zhao, X., Sun, H., Heimbrook, D.C., and Chen, L. (2006). Selective small-molecule inhibitor reveals critical mitotic functions of human CDK1. Proc Natl Acad Sci U S A *103*, 10660-10665.